Solvatochromic shift of phenol blue in water from a combined Car–Parrinello molecular dynamics hybrid quantum mechanics-molecular mechanics and ZINDO approach

N. Arul Murugan, Prakash Chandra Jha, Z. Rinkevicius, Kenneth Ruud, and Hans Ågren

Citation: The Journal of Chemical Physics **132**, 234508 (2010); doi: 10.1063/1.3436516
View online: http://dx.doi.org/10.1063/1.3436516
View Table of Contents: http://aip.scitation.org/toc/jcp/132/23
Published by the American Institute of Physics

Solvatochromic shift of phenol blue in water from a combined Car–Parrinello molecular dynamics hybrid quantum mechanics-molecular mechanics and ZINDO approach

N. Arul Murugan,[1,a)] Prakash Chandra Jha,[2] Z. Rinkevicius,[1] Kenneth Ruud,[2] and Hans Ågren[1]
[1]*Department of Theoretical Chemistry, School of Biotechnology, Royal Institute of Technology, SE-10691 Stockholm, Sweden*
[2]*Department of Chemistry, Centre for Theoretical and Computational Chemistry, University of Tromsø, N-9037 Tromsø, Norway*

(Received 18 March 2010; accepted 5 May 2010; published online 17 June 2010)

The present work addresses the solvatochromic shift of phenol blue (PB) dye. For this purpose the results of Car–Parrinello molecular dynamics (CPMD) simulations for PB in gas phase are compared with results obtained for PB in water from CPMD hybrid quantum mechanics-molecular mechanics (CPMD-QM/MM) calculations. The absorption spectra were obtained using the intermediate neglect of differential overlap/spectroscopic-configuration interaction (INDO/CIS) method and were calculated for a multitude of configurations of the trajectory. The calculated λ_{max} for PB in gas phase was found to be about 535 nm, which is considerably lower than the λ_{max} reported for PB in nonpolar solvents. Different solvation shells for PB in water have been defined based on the solute-all-atoms and solvent center of mass radial distribution function ($g(r_{X-O})$). The electronic excitation energies for PB computed in the presence of solvent molecules in an increasing number of solvation shells were calculated in a systematic way to evaluate their contributions to the solvatochrmic shift. The inclusion of solvent molecules in the hydration shell yields a λ_{max} of 640 nm, which contributes to almost 78% of the solvatochromic shift. The inclusion of solvent molecules up to 10 Å in the $g(r_{X-O})$ rdf yields a λ_{max} of 670 nm which is in good agreement with the experimentally reported value of 654–684 nm. Overall, the present study suggests that the combined CPMD-QM/MM and INDO-CIS approach can be used successfully to model solvatochromic shifts of organic dye molecules. © *2010 American Institute of Physics*.
[doi:10.1063/1.3436516]

I. INTRODUCTION

Solvatochromic molecules[1–4] have been used as molecular probes for revealing the nature of the micropolarity of many systems such as binary liquids, room temperature ionic liquids, supercritical liquids, and protein and polymer surfaces or cavities.[5–8] In order to obtain insight into the relationship between structure and absorption spectrum of the solvatochromic molecules and the solvatochromic shifts associated with their solvation in different solvents, an efficient and accurate model that takes into account the solute's microenvironment will be valuable. Such a model may contribute to our ability to design better solvatochromic molecular probes for protein characterization, as for instance suggested in Ref. 9. Trying to add to this picture, we propose and try out in this paper a sequential hybrid quantum mechanics-molecular mechanics (QM/MM) and ZINDO calculation technique for modeling of solvatochromic shifts of organic dyes, using phenol blue (PB) as the first testbed (see Fig. 1). A particular aim of the work is to understand the effect of solvation on the absorption spectra of PB in aqueous solution compared to gas phase. PB has been very useful as a solvatochromic probe for revealing the polarity of binary liquids,[10] supercritical CO_2,[11] room temperature ionic liquids,[8] and polyamidoamine (PAMAM) polymers.[12] The versatility of PB as a micropolarity probe owes to several reasons: (i) PB is smaller in size than mostly other solvatochromic probes, such as ET-30, and can therefore be used to infer the polarity around the cavity of a protein or a polymer. (ii) The absorption spectra of PB lie in the visible region, well separated from the absorbing regions of protein or polymers such as PAMAM dendrimers.[12]

PB has been studied using many experimental techniques, including IR, Raman, NMR, and pump-probe transient absorption measurements.[13–16] In particular, the spectroscopic properties of PB in different solvents (simple and binary mixtures) have been studied extensively.[17,18] PB appears to be one of the positive solvatochromic dyes (i.e., showing redshift in absorption spectra) that also display a large solvatochromic shift. The λ_{max} in nonpolar solvents such as n-hexane, cyclohexane ranges at 545–555 nm, while in water it shifts to a range of 654–684 nm.[15,17,18] Recently, we have performed Car–Parrinello (CP) hybrid QM/MM quantum mechanics molecular mechanics calculations to understand the molecular geometry of PB in gas-phase and in polar and nonpolar solvents.[19] We find that PB molecule remains in a neutral form in gas-phase and in chloroform sol-

a)Electronic mail: murugan@theochem.kth.se.

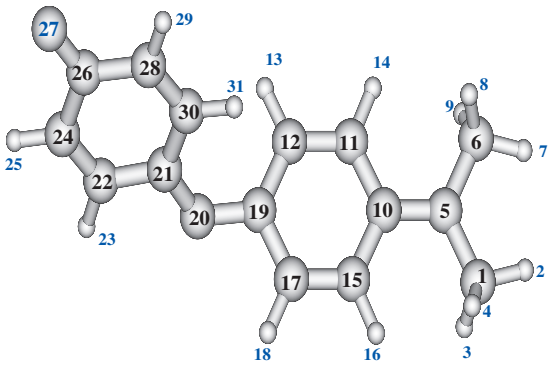

FIG. 1. The molecular structure of PB.

vent while it exists in a cyanine-like form in water solvent. The focus of the earlier study was on the solvent dependence of bond length alternation parameter, a structural parameter while in this paper we investigate the absorption spectra of PB in water solvent and its solvatochromic shift. The extensive use of PB as a solvatochromic probe and the rich experimental literature on the spectrum of PB makes this molecule an interesting target for studying in detail the solvation process on the solvatochromic shift.

Theoretical models to include solvent effects can be roughly categorized as either continuum or discrete models[20,21] The continuum models have their theoretical basis in the early ideas of Onsager[22] and Kirkwood[23] on enclosing the solute in a cavity that is surrounded by a polarizable dielectric continuum.[24–26] Although in many cases providing valuable insight into solvation processes, this is a rather crude model as the solvent is not considered explicitly. The model can therefore not describe specific interactions such as charge transfer between the solute and the solvent, nor hydrogen bonding between the solute and the solvent. Due to the presence of the OH, NO_2, and NH_2 functional groups in chromophores such as phenol blue, hydrogen bonds can be expected to be formed with protic solvents such as water, and a continuum model will therefore not be reliable for describing the solvation process in this case. The other approach, the "supermolecular approach," includes the solvent molecules explicitly (at least the solvent molecules that belong to the first solvation shell). A problem with this approach is that there often are a huge number of possible configurations to deal with for the solute-solvent supermolecule. To make the calculations possible, the property is therefore often calculated for the minimum energy configurations obtained from optimization[27] or for configurations selected from molecular dynamics, Monte Carlo (MC) or CP molecular dynamics (CPMD) simulations.[27–30] In the latter case, since the configurations are already weighted according to the Boltzmann distribution, the property calculated should correspond to the results obtained at a finite temperature. Overall, in the discrete models, an ensemble of solute-solvent supermolecular structures is obtained either from static or dynamic calculations. Absorption spectra of the solvated molecules can then be calculated for these configurations either using time-dependent density functional theory (TD-DFT) or more approximate methods such as the intermediate neglect of differential overlap/spectroscopic-configuration interaction (INDO/CIS) (Ref. 31) scheme as implemented in ZINDO.[32] Canuto *et al.* have successfully used a S-MC/QM procedure (refers to sequential MC and quantum mechanics) to model the solvatochromic shift of many organic molecules.[28,29,33] In this procedure, the ensemble of solute-solvent configurations are obtained from MC simulations, while the absorption spectra calculations are calculated using the INDO/CIS scheme. Recently, time-dependent density functional theoretical approaches have been implemented at the hybrid QM/MM level to model absorption spectra.[34–36] Overall, the S-MC/QM procedure appears very promising, as the method has proven its qualities in the calculation of solvatochromic shifts of organic molecules in both polar and nonpolar solvents,[28,29,37] being at the same time also computationally moderately demanding. For systems where the solvent-induced geometrical changes in the solute are significant,[38,39] this procedure may, however, have to be used with care. Going from gas phase to water solvent, results in a change of the twist angle by 26° in the case of *ortho*-betaine and the inclusion of flexibility contributes to as much as 4000 cm^{-1} in the solvatochromic shift as predicted by the simulations in Ref. 40. For such cases, one should either use *ab initio* MD calculations to treat the solvent-induced geometrical changes or the MC calculation should use a flexible molecular model in order to faithfully model these geometrical changes.

In this article, we use a combined CPMD/QM-MM and INDO/CIS procedure to model the solvatochromic shift of PB in water. We use the CPMD or CPMD-QM/MM procedure to get an ensemble of configurations at a finite temperature for PB in gas phase and in water solvent, respectively. The INDO-CIS scheme is then used to calculate the absorption spectra for PB in gas phase and in water solvent by a judicious selection of configurations from the trajectory. Due to the reasonable computational cost of INDO/CIS, we have tested the importance of including additional solvation shells in order to systematically analyze the contributions to the solvatochromic shift from solvent molecules in different solvation shells. We have used the solute-all-atoms and solvent center of mass radial distribution function (rdf) to define the different solvation shells around the PB molecule.

II. COMPUTATIONAL DETAILS

A. Car–Parrinello molecular dynamics calculations

A single PB molecule was optimized at the HF level using the 6-31G+(d,p) basis set using the GAUSSIAN03 software.[41] The optimized structure along with the General amber force-field[42] force-field has been used to define the PB for the initial MD calculations. The PB molecule has been solvated with 6526 water molecules in an orthorhombic box with a size of approximately, 63.4, 57.0, and 55.2 Å. The water molecules were described using the TIP3P force field.[43] The water molecules were allowed to equilibrate under ambient condition using MD calculations in an isothermal-isobaric ensemble for a time scale of 100 ps. The MD calculations were carried out using the SANDER module of the AMBER8 software.[44] The final configuration was used as the input configuration for the CP-QM/MM calculations. In our present calculations, we have used the Becke

exchange functional and the Lee, Yang, and Parr correlation functional as expressed in the BLYP gradient-corrected functional[45,46] and the Troullier–Martins norm-conserving pseudopotentials.[47] The electronic wave function is expanded in a plane wave basis set and the cutoff used was 80 Ry. We have used 5 a.u. as the time step for the integration of the equation of motion and 600 amu as the fictitious electronic mass. The calculations were carried out in a QM/MM setup,[48–51] where the PB molecule is treated using density functional theory, and the water solvent molecules are treated with a molecular mechanics force field (TIP3P). The QM/MM implementation used here includes the coupling between the QM part and the instantaneous electrostatic field arising from the dynamic MM environment. The interaction between the QM and MM systems involves electrostatic, short-range repulsion and long-range dispersion interaction terms (using the empirical van der Waals parameters). The CP-QM/MM calculations start with a quenching run that relaxes the initial structure within the QM/MM setup. The temperature scaling run was then carried out for 0.5 ps to rise the system temperature to 300 K. Finally, the system was connected to a Nose–Hoover thermostat and the length of the production run was 30 ps. For a comparative study of PB in solution phase with the gas phase, we have also carried out CPMD calculations on a single molecule of PB. The molecular geometry of the isolated PB molecule was optimized with the CPMD code[48] and subsequently the temperature scaling run and Nose production run were performed. The time scale used for the integration of the equations of motion during the scaling and Nose runs was 1 a.u., and the total time scale for the production run was 2 ps.

B. Calculations of absorption spectra

The aim of this work is to understand the solvent effects on the absorption spectra of PB. The spectra for PB in water and in gas phase were calculated using the INDO/CIS as implemented in the ZINDO module of GAUSSIAN03.[41] Studies in the literature comparing the TD-DFT and INDO-CIS schemes in reproducing the absorption spectra show that INDO-CIS many times can reproduce the experimental absorption spectra with an accuracy comparable to that of TD-DFT.[37] Indeed, in some cases the ZINDO with polarizable continuum model (PCM) appears to outperform the TD-DFT and TD-HF methods.[25] Furthermore, INDO-CIS calculations are not computationally expensive, and one can therefore be used to calculate the spectra for the solute molecule as well as a few hundred solvent molecules explicitly. It has been reported that the inclusion of solvent molecules (which interact with the solute molecule through specific bonds) is important to reproduce experimental spectra accurately.[25,37,52] Despite the documented qualities of the INDO-CIS approach, we have also performed DFT-PCM (B3LYP/Turbomole-pVDZ) calculations for comparison. The TD-DFT calculations were performed for a PB molecule and the water molecules in the first solvation shell, adding PCM outside the first solvation shell in order to model the solvent effect due to the more remote solvent molecules. The results obtained from this DFT-PCM level of theory gives a λ_{max} of 580 nm which is 80–100 nm away from the experimental data.[17,18] Moreover, due to inherent limitations of the system size, and nonavailability of standardized PCM parameters and identification of proper cavity radii, we decided to opt for the semiempirical ZINDO method. For PB in the gas phase, the calculations were carried out for around 130 configurations obtained from the 2 ps CPMD trajectory. For PB in water, 130 configurations were taken from the CPMD-QM/MM trajectory with a total simulation time of 30 ps. In this case, four different sets of calculations were performed. These calculations differ in the number of solvent molecules included in the calculations. First, we have calculated the solute-all-atoms and solvent center of mass rdf for PB in water. A detailed discussion about this rdf will be given in Sec. III. Based on the rdf, three different solvation shells were defined, and the calculations were carried out for the solute and the solvent molecules in the first, second, and third solvation shells, respectively. Beyond the third solvation shell, the density approaches unity, which is the bulk density. A fourth set of calculations have therefore also been carried out, in which the solute molecule and solvent molecules up to a distance of 10 Å were included. The transition energies are calculated for the different solute-solvent supermolecular clusters using the INDO/CIS model. In these calculations, the PB molecule includes 86 valence electrons and each water molecule includes eight valence electrons.

III. RESULTS AND DISCUSSION

A. Solvation shell structure of phenol blue in water

For the calculation of the absorption spectra of PB in water, we need to prepare the ensemble of solute-solvent supermolecular structures. Even though it can be expected that the solvent molecules far away from the solute molecules have smaller influence on the solute molecular geometry and its electronic properties, it is relevant to systematically investigate the effects of solvent molecules in different solvation shells on the solute's structural and electronic properties. The solvent molecules are usually arranged around the solute in different shells, sharing slow dynamics associated with solvent exchange between the shells, as has been studied extensively.[53,54] The solvation shell structure can be rationalized by calculating the rdfs involving all the atoms of the solute to the solvent molecules center-of-mass, and will be referred to as $g(r_{X-O})$. For nonspherical molecules, this rdf has been reported to be more relevant than the solute and solvent center of mass rdf.[55] We have also calculated the rdfs based on the minimum distance distribution functions between the other four solute atoms (such as O, N, C, and H) and the solvent center of mass. The results are shown in Fig. 2(a).

The calculated $g(r_{X-O})$ corresponds to the overall average of $g(r_{O-O})$, $g(r_{N-O})$, $g(r_{C-O})$, and $g(r_{H-O})$ rdfs. We can see a shoulder appearing in $g(r_{X-O})$ at a distance $r=3$ Å. A careful consideration of all the rdfs suggests that $g(r_{O-O})$ and $g(r_{H-O})$, and to a lesser extent $g(r_{N-O})$, contribute to this shoulder. We can define this shell as a hydration layer for the PB molecule as it includes all the solvents that are in immediate neighborhood to the PB molecule. We emphasize that

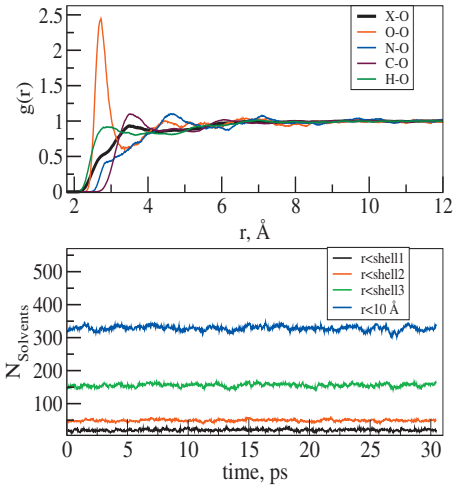

FIG. 2. (a) Solute-all-atoms and solvent center of mass rdf and other atom-atom rdfs, and (b) Time evolution of the number of solvent molecules in the different solvation shells.

not all water molecules in the hydration layer are hydrogen bonded to the solute PB molecule. We have not made any effort to identify the solvent molecules that are involved in hydrogen bonding and nor evaluated the contribution just from the hydrogen-bonded water molecules to the absorption spectra and hence to the solvatochromic shift.

If we further analyze the $g(r_{X-O})$ rdf, we can see a peak appearing between 3.0 and 4.3 Å. A comparison of this peak with $g(r_{C-O})$ suggests that the solvent molecules appearing at this distance range probably are in contact both with the water molecules in the hydration layer and with the C atoms of PB. At distances larger than 4.3 Å, we do not see any interesting feature in $g(r_{X-O})$ rdf, and beyond the distance 8 Å, the $g(r_{X-O})$ becomes unity, which means the solute does not influence the solvent structure beyond this distance. Based on the features seen in the $g(r_{X-O})$ rdf, we have defined different solvation shells in order to extract solute-solvent supermolecular clusters for the calculations of transition energies using ZINDO. The first solvation shell for PB includes the solvent molecules up to a distance of 3 Å in the $g(r_{X-O})$ rdf. The solvent molecules appearing up to 4.3 Å are defined as the second solvation shell, and similarly the solvent molecules up to a distance of 7.2 Å define the third solvation shell. Figure 2(b) shows the number of solvent molecules in the first, second and third solvation shells along with the number of solvent molecules appearing for distances $r < 10$ Å (which will be referred to as the fourth solvation shell).

The fluctuation in the number of solvent molecules (in different solvation shells) around a mean value shows that the structure of the solute-solvent supermolecular structures is equilibrated. The average number of solvent molecules is 20, 50, 156, and 330 for the first, second, third, and fourth solvation shells, respectively. An instantaneous configuration selected for PB and different solvation shells are shown in Fig. 3. Figure 3(a) shows an instantaneous configuration of the PB molecule and the solvent molecules in the first solvation shell. As described above, the figure shows that the PB molecule is involved in hydrogen bonding with solvent molecules through its nitrogen and oxygen atoms. Figures 3(b) and 3(c) show the PB molecule and the solvent molecules including the second and third solvation shells, respectively. Figure 3(d) shows the PB molecules and the solvent molecules included up to 10 Å in the $g(r_{X-O})$ rdf. These four figures show snapshots (at the same time) of the solute-solvent supermolecular structures used in the calculation of the absorption spectra.

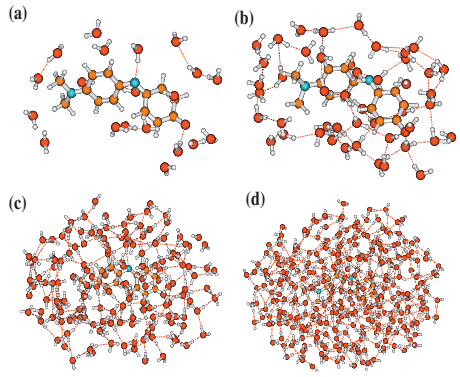

FIG. 3. Snapshots of PB in first, second, third, and fourth solvation shells.

B. Solvatochromic shift

In PB and in other solvatochromic molecules, the lowest excitation energy of π-π^* type has been reported to be associated with the solvatochromic shift.[1] The positive solvatochromic shift has been attributed to the stabilization of the excited state by more polar solvents compared to the ground state, since the excited state in these molecules is more polar. The excitation energy therefore decreases in more polar solvents resulting in a bathochromic shift or redshift. We have investigated the character of the frontier orbitals of PB in water and found that the highest occupied molecular orbital (HOMO) orbital is of π-orbital character. The lowest unoccupied molecular orbital (LUMO) is of π^* character as it has larger molecular orbital coefficients for the atoms of the phenol group. Figures 4(a) and 4(b) show the picture of the LUMO and HOMO orbitals for PB in water. The molecular orbitals shown are from a snapshot of PB and the first solvation shell water.

As the solvatochromic shift is associated with the lowest π-π^* transition, we will focus on this particular transition. Using the absorption spectra calculations carried out for many configurations (as discussed in Sec. II), the distribution of the excitation energy for the π-π^* transition has been calculated for both PB in gas phase and in water. The plots are shown in Fig. 5. The distribution curve is of Gaussian type and has been obtained from Eq. (1) (Ref. 56)

$$f(E) = \langle f \rangle \exp\left(- \frac{(E - \langle E \rangle)^2}{2\sigma_i^2} \right), \tag{1}$$

where $\langle f \rangle$ and $\langle E \rangle$ are the averaged oscillator strength and the averaged excitation energy, respectively, for the lowest excitation. Here, σ_i is the standard deviation in the lowest excitation energy calculated for all configurations in the trajectory. Overall, the distribution curve does not have any arbitrary parameters; the width of the curve is due to thermal

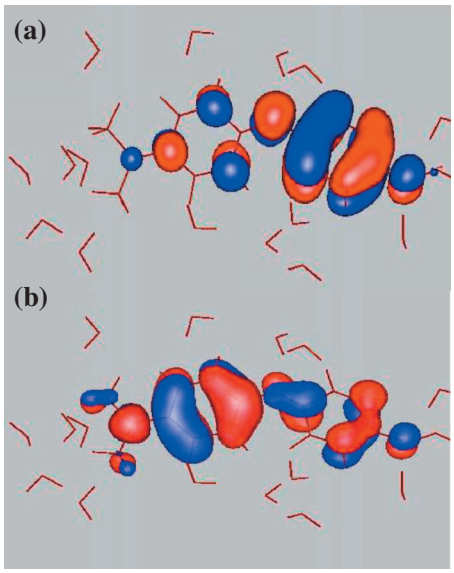

FIG. 4. (a) LUMO and (b) HOMO molecular orbital for PB-shell supermolecular system.

and solvents anisotropy in the solute-solvent system.

Figure 5 shows the excitation energy distribution curve for PB in gas phase and for PB with four different solvation shells. As the configurations have been generated from the CPMD calculations, the average excitation energy can be simply calculated by summing the excitation energy over all configurations

$$\langle E \rangle = \frac{\Sigma_{i=1}^{N} E_i}{N}, \tag{2}$$

where $\langle E_i \rangle$ is the excitation energy of an instantaneous configuration and N refers to number of configurations.

The calculated average excitation energies are reported in Table I. Here, we want to clarify that the distribution of excitation energy in Fig. 5 and the values in Table I show the cumulative contribution from solvation shells up to n. For example, shell-2 results include the contributions also from shell-1. The average excitation wavelength for PB in the gas phase is 535 nm. We are not aware of any experimental reports of the excitation energy for PB in gas phase. However, there are many reports on the absorption maximum reported for PB in nonpolar solvents such as hexane, cyclohexane, and benzene which can be used to compare with our gas-phase value.[1,17,18] Since the dielectric constant of these nonpolar solvents is close to 2, one may expect that the gas phase λ_{max} to reside lower when compared to λ_{max} reported in these solvents. The reported λ_{max} value in hexane is at 545–555 nm and in cyclohexane it is about 552 nm.[17,18] The theoretically calculated value for the absorption maximum in the gas phase of 535 nm appears to be comparable to these reported values.

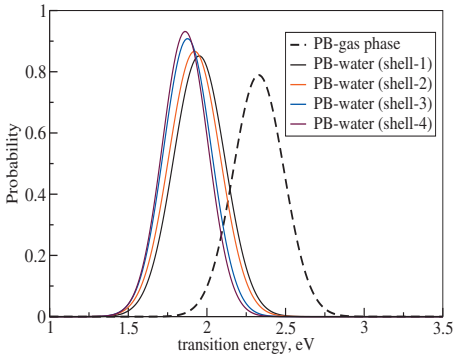

FIG. 5. The distribution of π-π^* excitation energies for PB in gas phase and in water.

TABLE I. Average excitation energies and solvatochromic shift obtained using the different computational models described in this paper.

System	π-π^* (nm)
PB gas phase	535
PB in nonpolar solvents (Expt.[a])	545–555
PB in water (shell-1)	640
PB in water (shell-2)	650
PB in water (shell-3)	665
PB in water (shell-4)	670
PB in bulk water (Expt.[a])	654–684
Solvatochromic shift	135

[a]References 17 and 18.

The experimentally reported absorption maximum for PB in water is 654–684 nm.[17,18] As we can see from Table I, the theoretical absorption maximum calculated for PB in water is in excellent agreement with these values. The inclusion of the water solvent molecules in the first hydration layer results by itself in a λ_{max} of 640 nm, which is in close agreement with the experimental observations [654–684 nm (Refs. 17 and 18)]. The inclusion of the water molecules in the hydration layer itself leads to a 105 nm solvatochromic shift in the absorption spectra. The second and third solvation shells contribute to a solvatochromic shift of 10 and 15 nm, respectively. The fourth solvation shell contributes only by 5 nm to the solvatochromic shift, which means that the effect of the solvent on the absorption spectrum has reached convergence. It was not possible to include solvent molecules beyond 10 Å, as the solute-solvent supermolecular structures in this case contains more than 510 water molecules and would require to include approximately 4050 valence electrons in the ZINDO calculation.

Overall the present calculations suggest that the inclusion of solvent molecules in the first hydration shell contributes about 78% to the solvatochromic shift. Our calculations validate the use of explicit water molecules in the hydration shell when modeling solvent effects on the absorption spectrum, since a major part of the effect can be recovered in doing so. A more accurate model will also have to include solvent molecules which are not involved in direct hydrogen bonding with the solute molecule. We have verified that the excitation energy is converged for PB in gas phase and in water. For this we have plotted the n-point average of the excitation energy as a function of number of configurations for both gas phase of PB and in water (see Fig. 6). We have also plotted the excitation energy corresponding to the instantaneous configurations. As we can see from the plots, the excitation energy has converged in both cases.

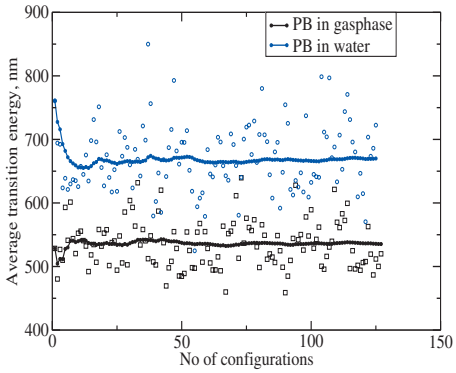

FIG. 6. Instantaneous and N-points average of first excitation energy calculated for PB in gas phase and in water.

IV. CONCLUSIONS

In the current work, we demonstrate that the combined use of CPMD-QM/MM and ZINDO calculations can be used to accurately predict the electronic excitation energy of PB in gas phase and in more polar solvents such as water. This procedure also allows us to systematically calculate the contributions from different solvation shells to the solvatochromic shift. Our calculations show that the inclusion of a single hydration shell recovers about 78% of the solvatochromic shift, and that the second and third solvation shell molecules contribute by about 7% and 11% nm to λ_{max}, respectively. Beyond the third solvation shell, the shift in the excitation energy is not very significant. The fourth solvation shell contributes only about 4% to the solvatochromic shift. Overall, the excitation energy for the PB in gas phase and in water has been reproduced accurately, and found to be in good agreement with available experimental reports.[17,18]

ACKNOWLEDGMENTS

This work was supported by a grant from the Swedish Infrastructure Committee (SNIC) for the project "Multiphysics Modeling of Molecular Materials," SNIC Grant No. 023/07-18. K.R. has been supported by the Research Council of Norway through a YFF Grant and a CoE grant (Grant No. 162746/V00). This work has also received support from NordForsk (Grant No. 179568/V30) and from the Norwegian supercomputer program through a grant of computer time.

[1] C. Reichardt, Chem. Rev. (Washington, D.C.) **94**, 2319 (1994).
[2] C. Reichardt, Org. Process Res. Dev. **11**, 105 (2007).
[3] C. Reichardt, D. Che, G. Heckenkemper, and G. Schafer, Eur. J. Org. Chem. **2001**, 2343 (2001).
[4] C. Reichardt, Angew. Chem., Int. Ed. Engl. **18**, 98 (1979).
[5] M. Y. Berezin, H. Lee, W. Akers, and S. Achilefu, J. Phys. Chem. B **93**, 2892 (2007).
[6] Y. Marcus, J. Phys. Org. Chem. **18**, 373 (2005).
[7] K. A. Fletcher, I. A. Storey, A. E. Hendricks, and S. Pandey, Green Chem. **3**, 210 (2001).
[8] T. Fujisawa, M. Fukuda, M. Terazima, and Y. Kimura, J. Phys. Chem. A **110**, 6164 (2006).
[9] A. Hawe, M. Sutter, and W. Jiskoot, Pharm. Res. **25**, 1487 (2008).
[10] O. W. Kolling and J. L. Goodnight, Anal. Chem. **45**, 160 (1973).
[11] J. Chen, D. Shen, W. Wu, B. Han, B. Wang, and D. Sun, J. Chem. Phys. **122**, 204508 (2005).
[12] D. L. Richter-Egger, J. C. Landry, A. Tesfai, and S. A. Tucker, J. Phys. Chem. A **105**, 6826 (2001).
[13] F. Terenziani, A. Painelli, and D. Comoretto, J. Phys. Chem. A **104**, 11049 (2000).
[14] T. Yamaguchi, Y. Kimura, and N. Hirota, J. Phys. Chem. A **101**, 9050 (1997).
[15] J. O. Morley and A. L. Fitton, J. Phys. Chem. A **103**, 11442 (1999).
[16] Y. Kimura, T. Yamaguchi, and N. Hirota, Phys. Chem. Chem. Phys. **2**, 1415 (2000).
[17] F. M. Menger and A. M. Sanchez, Chem. Commun. (Cambridge) **2**, 199 (1997).
[18] L. G. S. Brooker and R. H. Sprague, J. Am. Chem. Soc. **63**, 3214 (1941).
[19] N. A. Murugan, Z. Rinkevicius, and H. Ågren, J. Phys. Chem. A **113**, 4833 (2009).
[20] C. J. Cramer and D. G. Truhlar, Chem. Rev. (Washington, D.C.) **99**, 2161 (1999).
[21] V. Barone and A. Polimeno, Chem. Soc. Rev. **36**, 1724 (2007).
[22] L. Onsager, J. Am. Chem. Soc. **58**, 1486 (1936).
[23] J. G. Kirkwood, J. Chem. Phys. **2**, 351 (1934).
[24] S. R. Mente and M. Maroncelli, J. Phys. Chem. B **103**, 7704 (1999).
[25] M. Caricato, B. Mennucci, and J. Tomasi, J. Phys. Chem. A **108**, 6248 (2004).
[26] M. Caricato, B. Mennucci, and J. Tomasi, Mol. Phys. **104**, 875 (2006).
[27] W. Zhao, L. Pan, W. Bian, and J. Wang, ChemPhysChem **9**, 1593 (2008).
[28] K. Coutinho and S. Canuto, J. Chem. Phys. **113**, 9132 (2000).
[29] S. Canuto, K. Coutinho, and D. Trzesniak, Adv. Quantum Chem. **41**, 161 (2002).
[30] M. Parac, M. Doerr, C. M. Marian, and W. Thiel, J. Comput. Chem. **31**, 90 (2010).
[31] J. Ridley and M. C. Zerner, Theor. Chim. Acta **32**, 111 (1973).
[32] M. C. Zerner, ZINDO: A semiempirical program package, University of Florida, Gainesville (1999).
[33] K. Coutinho, N. Saavedra, A. Serrano, and S. Canuto, J. Mol. Struct.: THEOCHEM **539**, 171 (2001).
[34] M. Cascella, M. A. Cuendet, I. Tavernelli, and U. Röthlisberger, J. Phys. Chem. B **111**, 10248 (2007).
[35] U. F. Röhrig, I. Frank, J. Hutter, A. Laio, J. VandeVondele, and U. Röthlisberger, ChemPhysChem **4**, 1177 (2003).
[36] A. Osted, J. Kongsted, K. V. Mikkelsen, and O. Christiansen, Chem. Phys. Lett. **429**, 430 (2006).
[37] T. Andrade-Filho, H. S. Martins, and J. D. Nero, Theor. Chem. Acc. **121**, 147 (2008).
[38] R. Cammi, B. Mennucci, and J. Tomasi, J. Am. Chem. Soc. **120**, 8834 (1998).
[39] J. Gao and C. Alhambra, J. Am. Chem. Soc. **119**, 2962 (1997).
[40] N. A. Murugan and H. Agren, J. Phys. Chem. A **113**, 2572 (2009).
[41] M. J. Frisch, G. W. Trucks, H. B. Schlegel *et al.*, GAUSSIAN03, Revision C.02., Gaussian, Inc., Wallingford, CT, 2004.
[42] J. Wang, R. M. Wolf, J. W. Caldwell, P. A. Kollman, and D. A. Case, J. Comput. Chem. **25**, 1157 (2004).
[43] W. L. Jorgensen, J. Chandrasekhar, J. D. Madura, R. W. Impey, and M. L. Klein, J. Chem. Phys. **79**, 926 (1983).
[44] D. A. Case, T. E. Cheatham, C. L. Simmerling, J. Wang, R. E. Duke, R. Luo, K. M. Merz, B. Wang, D. A. Pearlman, M. Crowley, S. Brozell, V. Tsui, H. Gohlke, J. Mongan, V. Hornak, G. Cui, P. Beroza, C. Schafmeister, J. W. Caldwell, W. S. Ross, and P. A. Kollman, AMBER8, University of California, San Francisco, CA (2004).
[45] A. D. Becke, Phys. Rev. A **38**, 3098 (1988).
[46] C. Lee, W. Yang, and R. C. Parr, Phys. Rev. B **37**, 785 (1988).
[47] N. Troullier and J. L. Martins, Phys. Rev. B **43**, 1993 (1991).
[48] J. Hutter, M. Parrinello, D. Marx, P. Focher, M. Tuckerman, W. Andreoni, A. Curioni, E. Fois, U. Röthlisberger, P. Giannozzi, T. Deutsch, A. Alavi, D. Sebastiani, A. Laio, J. VandeVondele, A. Seitsonen, and S. Billeter, Computer code CPMD, version 3.11, Copyright IBM Corp. and MPI-FKF Stuttgart, 1990–2002.
[49] A. Laio, J. VandeVondele, and U. Röthlisberger, J. Phys. Chem. B **106**, 7300 (2002).
[50] A. Laio, J. VandeVondele, and U. Röthlisberger, J. Chem. Phys. **116**, 6941 (2002).
[51] R. Car and M. Parrinello, Phys. Rev. Lett. **55**, 2471 (1985).

[52] W.-G. Han, T. Liu, F. Himo, A. Toutchkine, D. Bashford, K. M. Hahn, and L. Noodleman, ChemPhysChem **4**, 1084 (2003).
[53] S. K. Pal, J. Peon, and A. H. Zewail, Proc. Natl. Acad. Sci. U.S.A. **99**, 1963 (2002).
[54] B. Bagchi, Chem. Rev. (Washington, D.C.) **105**, 3197 (2005).
[55] H. C. Georg, K. Coutinho, and S. Canuto, J. Chem. Phys. **126**, 034507 (2007).
[56] K. J. de Almeida, N. A. Murugan, Z. Rinkevicius, H. W. Hugosson, O. Vahtras, H. Ågren, and A. Cesar, Phys. Chem. Chem. Phys. **11**, 508 (2009).